Iraqi Journal of Science, 2026, Vol. 67, No. 8, pp: 4178-4195
DOI: 10.24996/ijs.2026.67.8.3

ISSN: 0067-2904

Removal of Color Pollutant from Wastewater Using Phragmites Australis and Sawdust as Biosorbents

Dunya Edan AL-Mammar[1], Noor Hussein AL-Shammari[1]*, Rasha Tariq Salim[2]
[1] Department of Chemistry, College of Science, University of Baghdad, Baghdad, Iraq
[2] College of Pharmacy, Uruk University, Baghdad, Iraq

Received: 28/1/2025 Accepted: 6/9/2025 Published: 30/ 8/2026

Abstract:
In this study, powders of Phragmites australis (Phm) and Sawdust (SD) were utilized as biosorbents to remove Rhodamine 6G (R6G) as a cationic dye from wastewater. The surface characteristics of these biosorbents were examined using atomic force microscopy (AFM) and Fourier transform infrared spectroscopy (FT-IR) before the adsorption experiments. The batch adsorption method was employed to investigate the influence of various factors, including the amount of Phm and SD powder, adsorption period, initial concentration of adsorbate, temperature, and pH that affected on the adsorption process. The results showed that the highest removal efficiency (R%)for R6G dye was found at an adsorbent weight of 0.16g, a concentration of 10 mg/L, an adsorption time of 30 min, and a pH of 7 for both SD and Phm. Adsorption isotherms at different temperatures were observed following L-type, and through the adsorption isotherm models used, it was found that the adsorption of R6G dye is better described by the Freundlich isotherm (FrI) model. Thermodynamic parameters analysis suggests that the adsorption process is endothermic in nature, spontaneous, and occurs with an increase in disorder for SD as adsorbent, while for Phm it is an exothermic process that occurs with a decrease in disorder. In addition, the adsorption of R6G dye onto both Phm and SD is of a physical adsorption type. The kinetic data were analyzed by pseudo 1st and pseudo 2nd models, and were found to follow a pseudo 2nd model with correlation coefficients (R^2 >0.9987and 0.9996) for Phm and SD, respectively. The study revealed that both SD and Phm represent potential low-cost biosorbents that effectively remove R6G dye from aqueous solutions.

Keywords: Adsorption, Rhodamine 6G (R6G), Phragmites australis (Phm), Sawdust (SD), Biosorbents, Adsorption isotherm, Thermodynamic, Kinetic.

إزالة الملوثات الملونة من مياه الصرف الصحي باستخدام قصب السكر ونشارة الخشب كمواد مازة حيوية

دنيا عيدان المعمار[1] , نور حسين الشمري[1]* , رشا طارق سالم[2]
[1]قسم الكيمياء , كلية العلوم , جامعة بغداد , بغداد, العراق
[2]كلية الصيدلة , جامعة اوروك , بغداد , العراق

الخلاصة
في هذه الدراسة، تم استخدام مسحوق قصب السكر (Phm) ومسحوق نشارة الخشب (SD) كممتزات حيوية لإزالة صبغة الرودامين 6G (R6G) كصبغة كاتيونية من مياه الصرف الصحي. تم تقييم خصائص

*Email: noor.aliewie1205@sc.uobaghdad.edu.iq

سطح الممتزات الحيوية باستخدام مجهر القوة الذرية (AFM) ومطيافية الأشعة تحت الحمراء (FT-IR) قبل إجراء تجارب الامتزاز. تم استخدام طريقة الامتزاز الدفعي لدراسة تأثيرعوامل مختلفة، المتضمنة وزن مسحوق Phm وSD، فترة الامتزاز، التركيز الابتدائي للممتز، درجة الحرارة، وقيمة الاس الهيدروجيني التي تؤثر على عملية الامتزاز. أشارت النتائج أن أقصى نسبة إزالة R% لصبغة R6G تم الحصول عليها عند وزن 0.16 جم، تركيز 10 مجم / لتر، وقت امتزاز 30 دقيقة ودرجة الاس الهيدروجيني 7 لكل من SD و Phm. لوحظت منحنيات الامتزاز عند درجات حرارة مختلفة تتبع النوع L، ومن خلال انموذجي الامتزاز المستخدمة وجد أن امتزاز صبغة R6G يوصف بشكل أفضل من خلال انموذج فيرندليش (Frl). يشير تحليل المعلمات الديناميكية الحرارية إلى أن عملية الامتزاز ماصة للحرارة بطبيعتها، تلقائية، وتحدث مع زيادة العشوائية بالنسبة لـ SD كمادة مازة، بينما بالنسبة لـ Phm فهي طاردة للحرارة تحدث مع انخفاض العشوائية وامتزاز صبغة R6G على كل من Phm وSD هو من نوع الامتزاز الفيزيائي. تم تحليل البيانات الحركية من خلال ألنماذج المنتحلة الأولى والثانية، ووجد أنها تتبع الأنموذج الحركي لتفاعل المرتبة الثانية المنتحلة مع معاملات ارتباط (R^2>0.9987 و0.9996) لـ Phm و SD على التوالي. كشفت الدراسة أن كل من SD و Phm يعتبران من المواد المازة الحيوية قليلة التكلفة والتي تزيل صبغة R6G بشكل فعال من محاليلها المائية.

1. Introduction

Dyes are extensively utilized across numerous industries, including, rubber, fabric, paper, plastic and cosmetics. Among these, the textile industry is the largest consumer of dyes, primarily for coloring textiles [1]. At present, the worldwide annual production of dyes exceeds 700,000 tons, with over 10,000 different commercial dyes available. It is estimated that approximately 2% of the total dye production is discharged directly into wastewater [2]. These coloured compounds are not only aesthetically displeasing, but also hinder light penetration and delay the activity of optical representation; for that, it is necessary to eliminate dyes from wastewater before emptying it. However, many dyes are carcinogenic, dangerous, and resistant to degradation, which seriously threatens human health and safety. Because of their high chemical and thermal stability, removing dyes from wastewater is a critical challenge. Various techniques have been employed for dye removal, including coagulation, reverse osmosis, electrocoagulation, biological treatment, ion exchange, advanced oxidation, and biosorption using natural materials [3]. Among these technologies, adsorption has proven to be more versatile and effective than other techniques for treating wastewater, offering advantages such as ease of operation, initial cost, lack of sensitivity to toxic materials, simplicity of design, and removing full dyes even from dilute solutions [4]. Low-cost alternative adsorbents with high adsorption capacity are used to remove dyes wastewater, for example, sawdust (SD), bagasse pith, wood, fly ash, soil, peat, waste coir pith, china clay, banana pith and Phragmites australis [5]. Dyes are usually classified by function groups or colour and structural, and by ionic charge upon dissolution in aqueous solution. They are classified into nonionic and ionic dyes. Ionic dyes are classified into anionic dyes (direct, reactive, and acidic dyes), and cationic dyes (basic dyes), while nonionic dyes are further classified into disperse dyes and vat dyes. Because the classification of dyes strongly affects the adsorption efficiency of dyes [6]. Rhodamine 6G dye is one of the fresh peaches synthetic dyes and is widely used as a coloring agent in textile and food production. It has been medically proven that drinking water contaminated with Rhodamine dyes can cause subcutaneous sarcomas, which are highly carcinogenic. In addition, other types of toxicity from exposure to these dyes, such as reproductive toxicity and neurotoxicity, have also been extensively and intensively investigated and proven [7]. Various natural and waste materials have been extensively explored and studied to adsorb and remove various contaminants from aqueous solutions. Phm was used as an adsorbent for the removal of various dyes after chemical and thermal modification [8,9]. Furthermore, SD plays a chief

role in the removal of pollutants from wastewater because it has numerous functional groups, and it can be activated or modified by alkali and acid to enhance its adsorption potential to remove dyes as effluents [10,11].

In this study, Sawdust and Phragmites were employed as low-cost biosorbents to remove R6G dye from aqueous solution. The characteristics of the adsorbents were analysed using AFM and FT-IR. Additionally, the research investigated the optimal equilibrium adsorption conditions, including adsorbent amount, adsorption period, dye concentration, temperature, and pH. Isothermal models, thermodynamic parameters and kinetic models using pseudo 1st and pseudo 2nd models.

EXPERIMENTAL

2. Materials and Methods

2.1. Materials

Adsorbents:

Phragmites australis (Phm), commonly known as reeds, is one of the most widespread species that are often found around lakes, rivers and tables. Due to its characteristics such as ease of availability, low cost and tremendous productivity, Phm holds significant potential as an effective material for removing liquid waste sources for chemicals and biofuels [12]. Sawdust (SD) is a secondary product of the wood industry that is used either as packing material or fuel for cooking [5]. Because it contains many function groups that include amide groups, hydroxyl, carboxyl and phenolic in its structure, which may be suitable for adsorption of a large variety of dyes [13]. The biosorbents were collected and washed several times with warm distilled water to remove the dust and soluble constituents, and oven-dried at 60ºC for 24 hours. Then, the dried substances are ground to a fine powder using a mortar and pestle and finally dried at 100 ºC (2 hours). The dried powder was stored in a desiccator until it was used as an adsorbent in the adsorption experiments.

Adsorbate:

Rhodamine 6G: R6G dye used in this study is a cationic dye. Chemical formula is $C_{28}H_{31}ClN_2O_3$ and Colour Index is (CI) 45160, with IUPAC name [9-(2-ethoxy carbonyl phenyl)-6-(ethylamino)-2,7-dim-ethylxanthen-3-ylidene]-ethylazanium chloride) [14]. The chemical structure of the R6G molecule is illustrated in Figure 1. A stock solution of R6G dye at 1000 mg/L was prepared by dissolving 1g of R6G dye in distilled water (1000ml). This stock solution is diluted to prepare various concentrations of R6G dye for adsorption experiments. To determine the dye concentration at equilibrium, a calibration curve was established (Figure 2) using various concentrations ranging from 5 to 50 mg/L. The absorbance of the solution was measured with a UV-Visible spectrophotometer at λ_{max} equal to 524 nm.

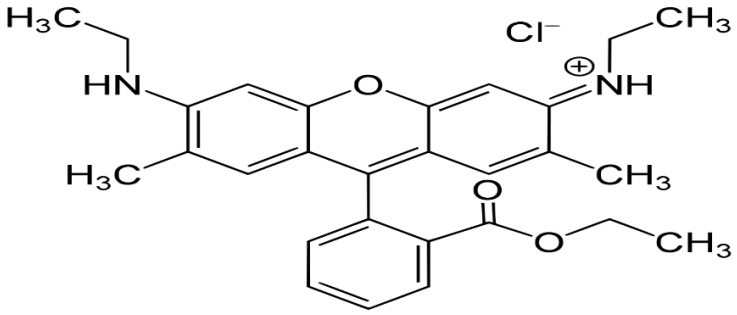

Figure 1: Chemical structure of Rhodamine 6G (R6G) dye**.**

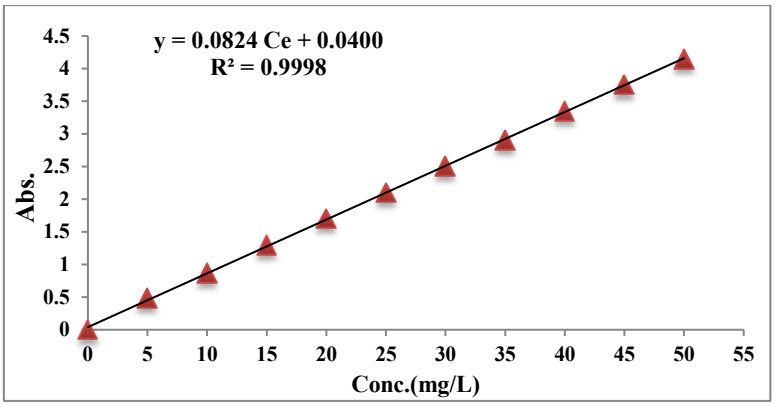

Figure 2: Calibration Curve of Rhodamine 6G dye at (λ_{max}=524)

2.2. Batch Adsorption Method

Adsorption experiments were performed to determine the optimum conditions for the removal of R6G using SD and Phm as adsorbents. These tests were carried out in a SHA-B water bath thermostat oscillator set at 298 K with a shaking speed of 150 rpm. The effect of the biosorbents amount was studied by varying the amount of SD and Phm from 0.04g to 0.24g, with a dye concentration of 10 mg/L and a volume of 25mL of solution for 30 min. The impact of the adsorption period was investigated by varying times (5 to 90 min), with an adsorbent amount of 0.32g/50mL dye solution and concentration (10mg/L). To study the impact of the R6G dye, different concentrations ranging from 5mg/L to 25mg/L were prepared, with 0.16g/25mL of R6G dye for 30 min. Residual R6G dye concentration was measured with a UV-Vis Spectrophotometer (Shimadzu UV 1800, Japan). R% removal efficiency and amount at equilibrium of adsorbed dye q_e (mg/g) were calculated using the following relationships [15]:

$$q_e = \frac{c_i - c_e}{m} \times v \quad \text{..... (1)}$$

$$R\% = \frac{c_i - c_e}{c_i} \times 100 \quad \text{..... (2)}$$

Where:

v: Volume of the solution (L).

$\mathbf{c_e}$: Concentration of dye (mg/L) at the equilibrium.

$\mathbf{c_i}$: Initial dye concentration(mg/L).

m: Weight of adsorbents (g).

2.3. Adsorption Isotherm

2.3.1. Langmuir Isotherm (LI) Model: This model is suitable for mono-layer adsorption on the surface and not desorbing adsorbate at the surface level. Therefore, **(LI)** model linear is given by**:**

$$\frac{C_e}{Q_e} = \frac{1}{K_L Q_m} + \frac{1}{Q_m} . C_e \quad \text{..... (3)}$$

Where:

$\mathbf{Q_m}$: Maximum capacity (mg/g) of the mono layer coverage.

$\mathbf{K_L}$: Langmuir constant (L.mg^{-1}).

$\mathbf{Q_e}$: Amount of adsorbed material per gram (mg. g^{-1}) of the adsorbent at equilibrium.

Values of $\mathbf{R_s}$ a separation factor or dimensionless constant is expressed as**:**

$$R_s = 1/ (1 + K_L C_i) \quad \text{..... (4)}$$

Values of R_s lies between (0,1) indicates that adsorption is sufficient, linear $R_s = 1$, favorable $1 > R_s > 0$, Irreversible $R_s = 0$ and unfavorable $R_s > 1$**.**

2.3.2. Freundlich Isotherm (FrI) Model: According to **(FrI)** model, the surface of the adsorbent is heterogeneous, as well as multilayer adsorption. The (**FrI**) model linear equation is expressed as**:**

$$\ln q_e = \ln K_{Fr} + \left(\frac{1}{n_f}\right) \ln C_e \quad \text{..... (5)}$$

Where:

$\mathbf{K_{Fr}}$: (**FrI**) constant ($mg.g^{-1}(mg.L^{-1})^{-1/n}$) is related to the adsorption capacity.

$\mathbf{n_f}$: Freundlich exponent.

When it ($1/n_f$ =1) The adsorption curve is linear, which indicates that there is no interaction between adsorption sites and the adsorbed species are homogeneous type. When ($1/n_f$> 1) the adsorption is unfavorable, the adsorption capacity decreases, and the adsorption bonding becomes weaker, when (1> $1/n_f$>0), the adsorption is favorable and thence adsorption capacity increases [16].

2.4. Adsorption Thermodynamics:

Thermodynamic parameters are used to evaluate the spontaneity and assess the degree of randomness in an adsorption process. The values of standard Gibbs free energy change (ΔG°), standard enthalpy change (ΔH°), and standard entropy change (ΔS°), were calculated using the following equations [17**]:**

$$K_{eq} = \frac{C_i - C_e}{C_e} [V/m] \quad \text{..... (6)}$$

$$\Delta G° = -RT\ln K_{eq} \quad \text{..... (7)}$$

$$\Delta G° = \Delta H° - T\Delta S° \quad \text{..... (8)}$$

Where:

T: Absolute temperature (K).

R: Gas constant (8.314 J/mol.K).

$\mathbf{K_{eq}}$: Equilibrium constant of the adsorption.

The values of ΔH° and ΔS° can be obtained from the slope and intercept respectively of a plot $\ln K_{eq}$ versus 1/T in the Van't Hoff equation**:**

$$\ln K_{eq} = \frac{\Delta S°}{R} - \frac{\Delta H°}{RT} \quad \text{..... (9)}$$

2.5. Kinetic Model

To illustrate the kinetics of R6G adsorption onto the both adsorbents, two kinetic models are utilized: Pseudo-First order model (Pseudo 1st model), Pseudo-second order model (Pseudo 2nd model). These two models are written based on the following equations:

$$\ln (q_e - q_t) = \ln q_e - k_1.t \quad \text{..... (10)}$$

$$\frac{t}{q_t} = \frac{1}{k_2 q_e^2} + \frac{t}{q_e} \quad \text{..... (11)}$$

Where:

$\mathbf{q_t}$: adsorbed amount ($mg.g^{-1}$) of adsorbate onto adsorbent at a time.

$\mathbf{k_1}$: rate constant (min^{-1}) for the pseudo 1stmodel

$\mathbf{q_e}$: equilibrium adsorption capacity ($mg.g^{-1}$)

$\mathbf{k_2}$: the equilibrium rate constant (g/mg.min) for a pseudo 2nd model.

The slopes and intercepts of the linear plots of ln ($q_e - q_t$) versus (t) and (t/q_t) versus (t) were applied to estimate the values of k_1 , q_e for the pseudo 1st and values of k_2 , q_e for pseudo 2nd **[**18].

3. Results and Discussions

3.1. Adsorbents Characterization

3.1.1. Atomic Force Microscopy (AFM)

AFM apparatus type (AA3000, angstrom Advanced Inc., USA) was used to display mean grain size measurements. AFM is used to study the shape, topography of surface roughness, size and orientation of adsorbed surfaces. Of particular interest in these studies are soft imaging and force curves that explore the utilization of surface layer properties. The average diameters for SD is 91.5 nm and Phm is 925.4 nm. Figures 3 and 4 show a typical surface obtained from 3D AFM images and the cumulative distribution of adsorbents. This indicates that the particle size of SD is smaller than that of Phm, which leads to an increase in the specific surface area for SD. The images obtained for SD show parallel-oriented fiber structures (Figure 4), with a relatively fine-grained structure. The average grain size was found to be 91.5 nm. This suggests that the circular features observed are the result of fiber cutting during the formation of SD particles [19]. In addition, Phm exhibits a significantly larger average grain size of 925.4 nm, which contributes to a more inhomogeneous surface. This is likely due to the presence of large aggregates composed of lignocellulose and phenolic compounds, covered by a layer of non-cellulosic wax [20].

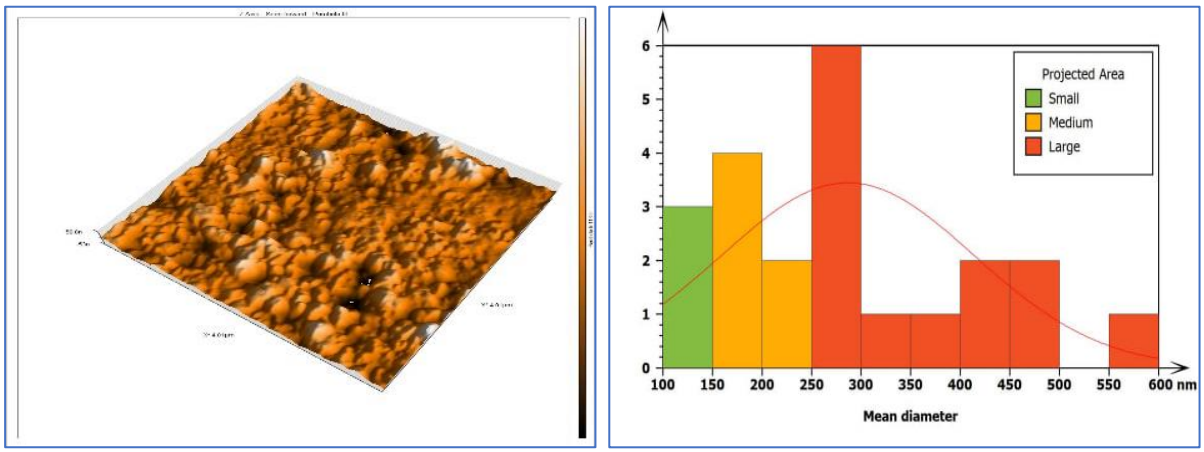

Figure 3: 3D view of AFM images and granularity cumulating distribution chart of SD powder.

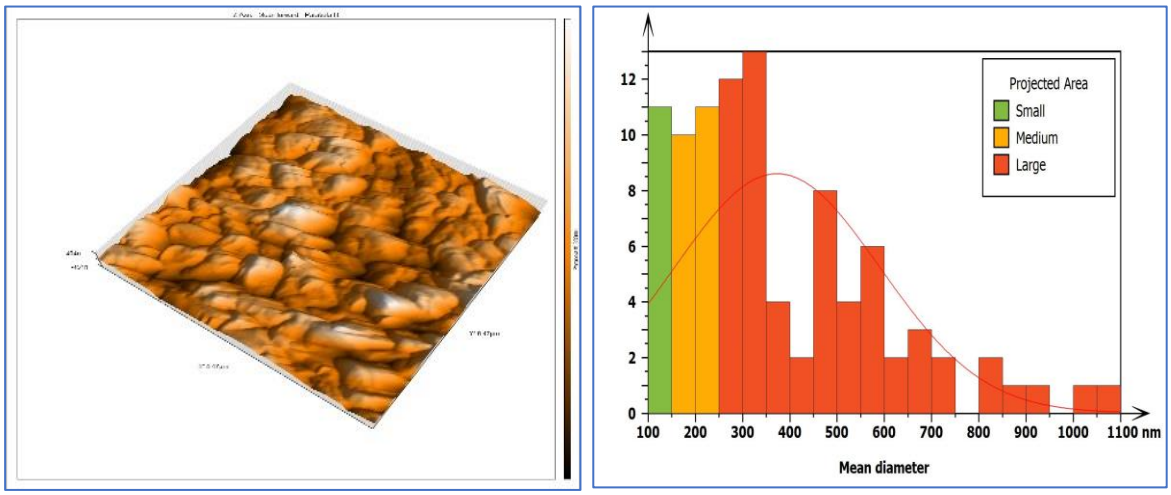

Figure 4: 3D view of AFM images and granularity cumulating distribution chart of Phm powder.

3.1.2. Fourier Transform Infrared Spectroscopy (FT-IR)

FT-IR spectra were scanned over a wavelength range from 400 to 4000 cm^{-1} at 25ºC. The characteristic bands for SD and Phm are shown in Figures **5** and **6**. FTIR spectroscopy applied to SD and Phm lies in its ability to characterize the functional group and fingerprint region of samples. SD and Phm samples show a broad band in the 3600-3200 cm^{-1} region associated with the stretching of hydroxyl groups (O-H) and a broad band in the 3000-2800 cm^{-1} region associated with the stretching of C-H. The wavenumber of carbon dioxide is 2400-2260 cm^{-1} for Phm sample [21]. While the band intensity was about 1720 and 1703 cm^{-1} for SD and Phm, respectively, related to carbonyl group C=O stretching. The observed peaks in the wave number range of 1650-1550 cm^{-1} correlated to N-H primary amines, 1450-1400 cm^{-1} attributed to C=O carboxylic acids, 1080-1050 cm^{-1} belonging to C-O primary alcohols, 1090-1000 cm^{-1} correspond to C-O esters, and 800-700 cm^{-1} related to mono-substituted aromatics. The bands occurring at frequencies between 700 and 400 cm^{-1} are characteristic of the C-H groups of cellulose [22]. The identified hydroxyl (–OH) and carbonyl (C=O) groups are not only structural indicators but also act as active sites for hydrogen bonding and electrostatic interactions with the cationic Rhodamine 6G dye, thereby enhancing adsorption efficiency [23].

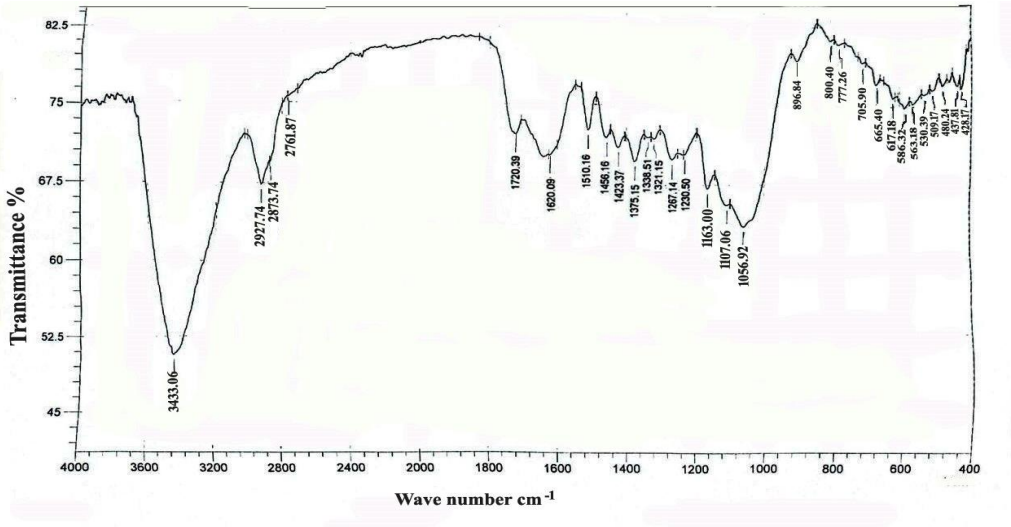

Figure 5: FTIR analysis of SD powder.

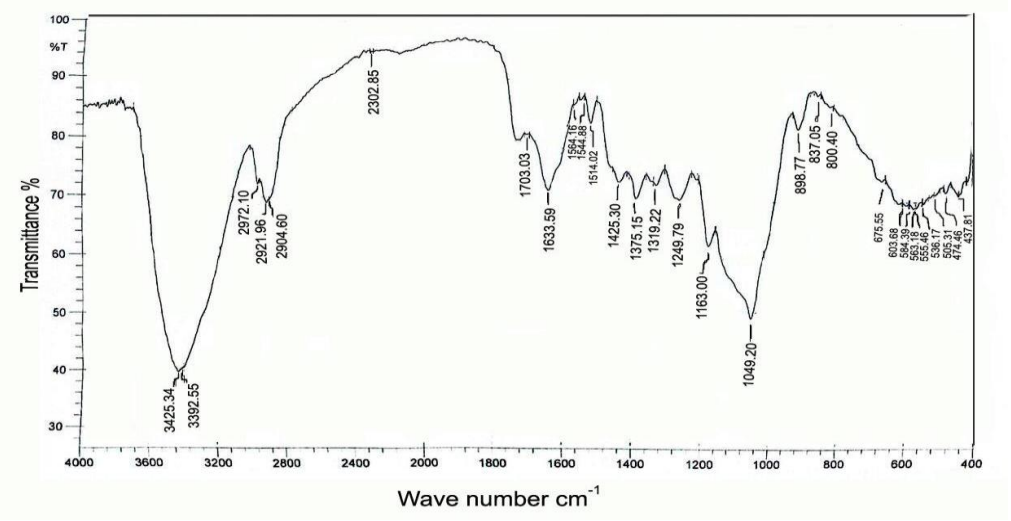

Figure 6: FTIR analysis of Phm powder.

3.2. Adsorption Experiments

3.2.1. Adsorbent Amount Effect:

Figure 7 presents the effect of adsorbent dosage (0.04–0.24 g) on the removal of R6G dye using SD and Phm powder. The experiments were conducted with 25 mL of a 10 mg/L dye solution at pH 7, 298 K, 150 rpm for 30 minutes. It is obvious from this Figure that R% increased from 48.6% to 90.6% for SD and 34.0% to 82.5% for Phm. The increase in the removal of the R6G dye with an increase in the dose of adsorbents was expected because of the increased number of active sites available for the adsorption process [24]. Moreover, the use of SD as an adsorbent exhibited a higher removal efficiency for R6G dye compared to Phm, this may be related to the smaller particle size of SD, which results in an increased surface area available for interaction with dye molecules. As we notice the removal ratio is nearly constant from 0.16g to 0.24g, therefore, the optimum weight of the adsorbents is 0.16 g.

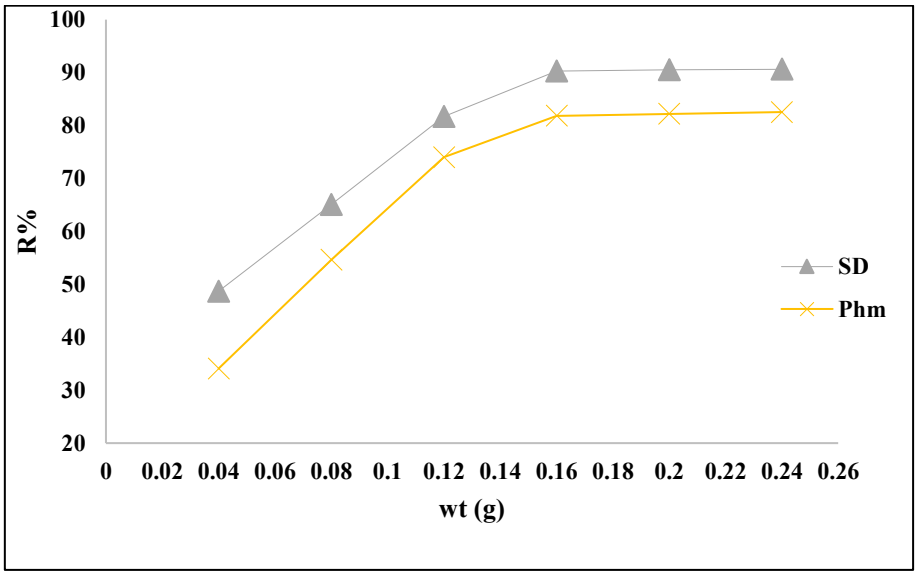

Figure 7: Effect of biosorbent dosage on the removal efficiency (R%) of R6G dye using SD and Phm powders at 25 °C, 10 mg/L dye concentration, 30 min contact time, pH 7).

3.2.2. Effect of Adsorption period:

The period of the adsorption was varied from 5 to 90 minutes under the following conditions: amount of adsorbent (0.32g / 50 ml), initial concentration (10 mg/L), shaking speed (150 rpm) at 298K and pH 7. The results are shown in Figure 8. The maximum adsorption was reached at 30 min, with no notable increase in removal percentage observed beyond this time. The rise in %R with longer adsorption times can be attributed to the fact that more time becomes available for dye ions to make an attractive complex with surface biosorbents [25]. After 30 min the removal percentage remains constant, which can be attributed to the saturation of the majority of active sites on the surface of the adsorbents, indicating that equilibrium had been achieved.

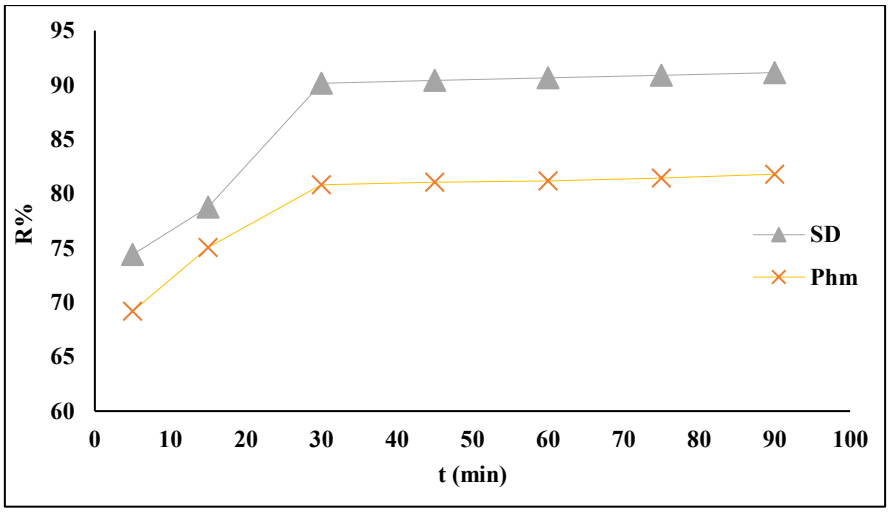

Figure 8: Effect of contact time on R6G dye removal efficiency (R%) using SD and Phm biosorbents under standard conditions (298 K, 10 mg/L R6G, 0.32 g adsorbent/50 mL, pH 7).

3.2.3. Effect of Initial R6G Dye Concentrations:

Figure **9** shows the impact of initial concentrations of R6G dye onto biosorbents with the following conditions: adsorption period 30 minutes, amounts of adsorbent 0.16 g/ 25 ml, shaking speed (150 rpm) at 298K and pH 7. When the initial concentration of dye is increased from 5 to 25 mg/L, the R% decreases from 91.6 to 75.7% for SD and from 81.2 to 68.4% for Phm. This may be since at higher concentrations of R6G dye, the surface of the biosorbent is rapidly saturated and nearly all dye molecules diffuse slowly through the pores, but at low concentrations, most dye molecules are adsorbed to the surface [26]. Therefore, the optimum concentration was set at 10 mg/L.

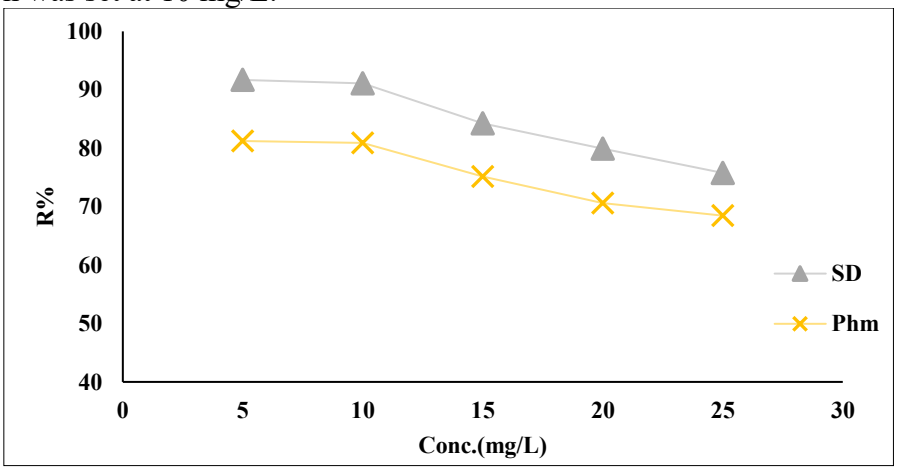

Figure 9: Impact of initial concentrations for the adsorption of R6G dye onto SD and Phm powder under standard conditions (298 K, 30 min contact time, 0.16 g adsorbent/25 mL, pH 7).

3.2.4. Temperature Effect:

The temperature effect is very important in the adsorption process, as it helps in determining the exothermic and endothermic nature of the adsorption process**.** The temperature impact on the removal percentage of R6G dye is performed in the temperature range of 288-328 K, R6G concentration 10mg/L, amount of adsorbent 0.16 g/25 ml, adsorption period 30 min, shaking speed 150 rpm and pH 7. Figure 10 shows that R% values decrease with increasing temperature for Phm. This inverse relation between R% and temperature indicates that the adsorption process is exothermic, accompanied by a weak physical bonding between the active sites of Phm powder and dye molecules [27]. For SD, the

removal percentage (R%) rose as the temperature increased. Therefore, the adsorption process can be classified as an endothermic process; this may be related to an increase in the active sites for the adsorption and the increase in the mobility of the dye molecules with increasing temperature [11].

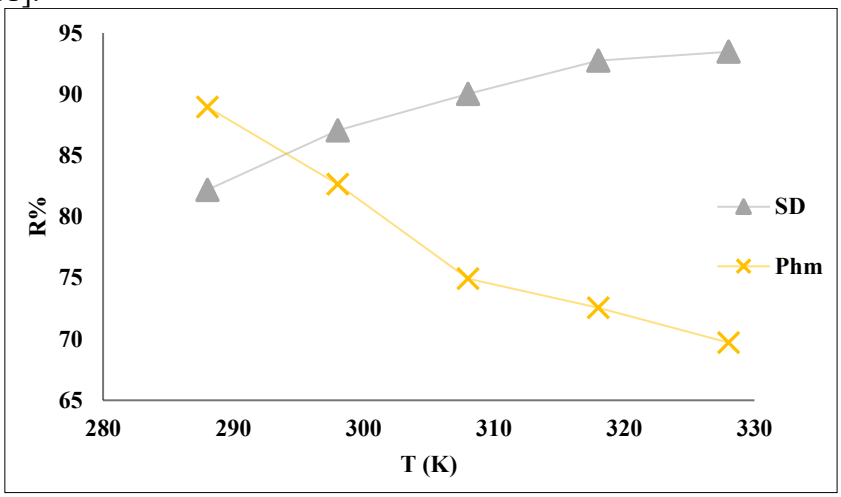

Figure 10: The temperature effect for the adsorption of R6G dye onto SD and Phm powder under standard conditions (10 mg/L R6G, 30 min contact time, 0.16 g adsorbent/25 mL, pH 7).

3.2.5. Influence of Initial pH

Influence pH of the solution is a very important parameter for adsorption. pH of the solution not only affected the dissociation of the surface charge of the adsorbents and functional groups on the active sites of the adsorbents, but also the structure of the dye molecule [28]. The influence of pH solution on the adsorption of R6G was investigated in the pH range from 2.0 to 12.0, at 298K for 30 minutes, amount of adsorbent of 0.16 g/ 25 ml, R6G concentration 10mg/L and shaking speed 150 rpm. Figure 11 shows R% increases with increasing pH from 21.2% to 91.0% for Phm and from 28.5% to 94.2% for SD. The removal percentage of R6G dye increases with increasing solution pH from 2 to 7, and remains almost unchanged when further increasing the solution pH. This can be explained as in the case of cationic dyes at low pH value, H^+ ions will compete with the dye cations, causing the R% to decrease. On the contrary, the higher the pH values, the more negatively charged the surface becomes, creating an attractive force between the positively charged dye molecules and the biosorbents that leads to improving the adsorption process [29]. Additionally, the surface functional groups like hydroxyl (-OH) and carboxyl (-COOH) undergo protonation or deprotonation depending on the pH level of the solution. At acidic pH, these groups tend to be protonated, which decreases the negative charge on the biosorbent surface and weakens electrostatic interactions with the positively charged dye molecules. As the pH rises, deprotonation occurs, resulting in more negatively charged sites on the surface that enhance the attraction and binding of cationic dyes such as R6G [30]. The selected pH was 7 for further experiments.

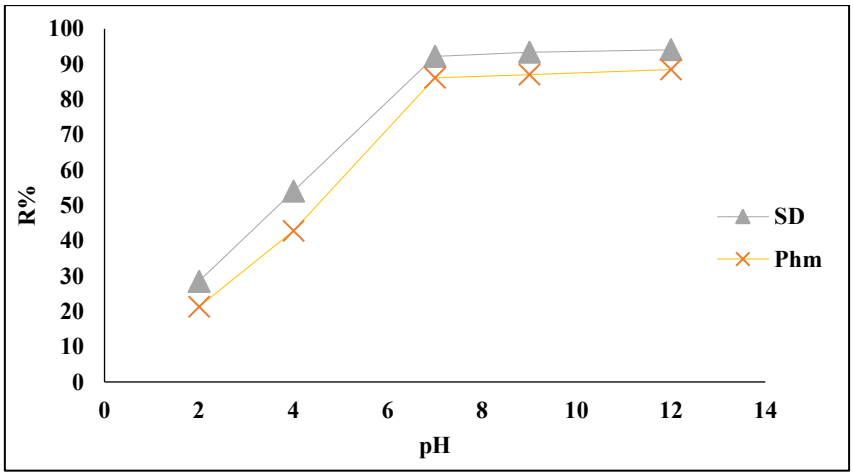

Figure 11: Impact of initial pH for the adsorption of R6G dye onto SD and Phm powder under standard conditions (298 K, 10 mg/L R6G, 30 min contact time, 0.16 g adsorbent/25 mL)

3.3. Adsorption Isotherms

The models of adsorption isotherms can describe the interactions between the adsorbent surface and the adsorbate**.** Table 1 shows the values of q_e and C_e for the adsorption of R6G dye at different temperatures. Adsorption isotherm experiments were performed at five various temperatures as 288, 298, 308, 318 and 328 K, with a weight of the biosorbents was 0.16g/25 mL, an adsorption time was 30 min, a shaking speed of 150 rpm, and different concentrations of R6G dye ranged 5,10,15,20,25 mg/L/L. Figure 12 shows the adsorption isotherms for the adsorption of R6G dye onto SD and Phm powder. From these Figures, it was predicted that according to Giles classification, the adsorption process follows L-type isotherm, which type is based on curvature, and the initial slope of the isotherm curves of adsorbates has a strong affinity for the adsorbent [31]. When the active site of the substrate fills up, it becomes difficult for the solvent molecule to find a free site. As the solvent concentration increases, the adsorption capacity increases until the active sites are filled, the equilibrium adsorption capacity of the adsorbent reaches a maximum value, and the adsorption capacity rapidly decreases when the volume of monolayer formation (plateau) is reached [32].

Table 1: Values of C_e and q_e For the adsorption of R6G dye onto biosorbent samples at various temperatures.

	288K		298K		308K		318K		328K	
C_i mg/L	C_e mg/L	q_e mg/g	C_e mg/L	q_e mg/g	C_e mg/L	q_e mg/g	C_e mg/L	q_e mg/g	C_e mg/L	q_e mg/g
SD										
5	1.2621	0.5840	0.4733	0.7072	0.2912	0.7357	0.1577	0.7565	0.0970	0.7660
10	1.8203	1.2780	1.3228	1.3558	1.0194	1.4032	0.7402	1.4468	0.6674	1.4582
15	3.2281	1.8393	2.4150	1.9663	2.0995	2.0157	1.7111	2.0763	1.3349	2.1351
20	4.8300	2.3702	4.1019	2.4840	3.6165	2.5599	3.1796	2.6281	2.5606	2.7248
25	7.0752	2.8007	6.1893	2.9391	5.2791	3.0813	4.8422	3.1496	4.1868	3.2520
Phm										
5	0.5461	0.6959	0.7402	0.6655	1.1286	0.6049	1.4441	0.5556	1.7961	0.5006
10	1.2500	1.3671	1.7718	1.2856	2.5606	1.1623	2.8034	1.1245	3.0946	1.0789
15	2.9854	1.8773	3.4587	1.8033	4.0291	1.7141	4.8058	1.5928	5.3277	1.5113
20	4.9029	2.3589	5.7039	2.2338	6.5048	2.1086	7.5000	1.9531	8.2039	1.8431
25	6.4563	2.8975	7.7549	2.6946	8.6286	2.5580	9.7573	2.3817	10.631	2.2451

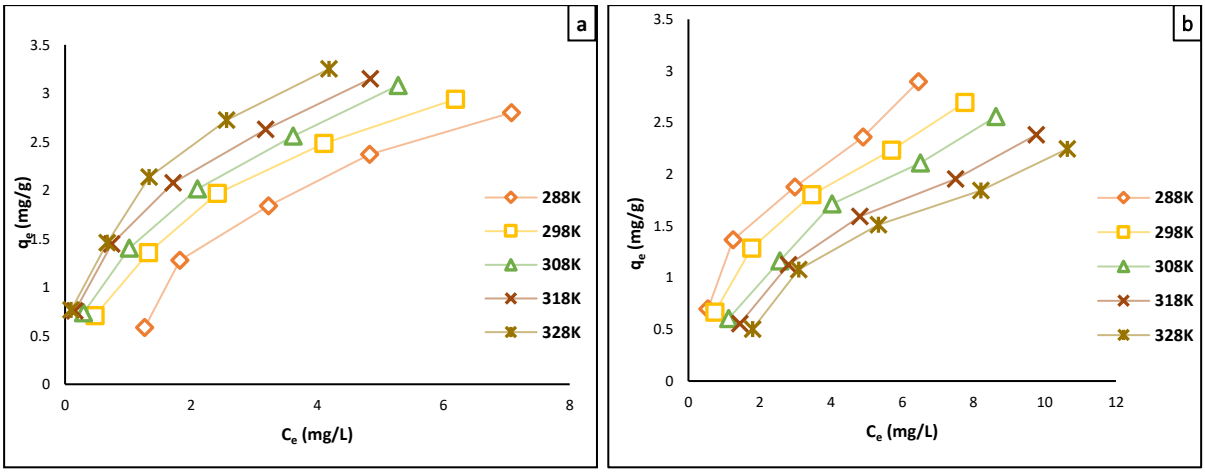

Figure 12: Adsorption isotherms for the adsorption of R6G dye onto (a) SD (b) Phm at various temperatures.

3.3.1. Langmuir Isotherm (LI) Model:

Figure 13 presents the **LI** plots for the adsorption of R6G dye onto biosorbents. The values of the maximum of mono-layer capacity Q_m (mg/g), correlation coefficient R^2, Langmuir constant K_L, and the separation factor R_S were presented in Table 2. Where the R^2 values were found to be between 0.4421-0.9944 for SD and 0.7636-0.9873 for Phm. Hence, this model is not appropriate, and the R_S values for SD decreased from 0.3467 to 0.0305 at high temperatures, which indicated that adsorption was more favorable at high temperatures. Conversely, the R_S values for Phm decreased from 0.3792 to 0.0936 at low temperatures, indicating that adsorption is more favorable at low temperatures [33].

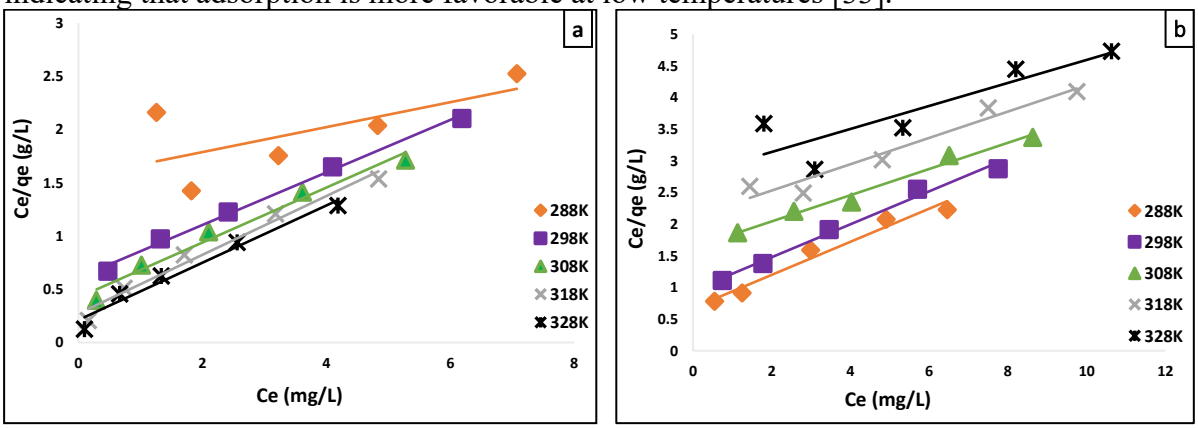

Figure 13: (LI) plots for the adsorption of R6G dye onto (a) SD (b) Phm at various temperatures.

Table 2: K_L and R_S values for adsorption of R6G dye onto SD and Phm at various temperatures, C_i (10 mg/L)

Temperature (K)	SD				Phm			
	Q_m ($mg.g^{-1}$)	K_L (L/mg)	R^2	R_S	Q_m ($mg.g^{-1}$)	K_L (L/mg)	R^2	R_S
288	8.5397	0.0753	0.4421	0.3467	3.8255	0.3869	0.9653	0.0936
298	4.0535	0.4040	0.9944	0.0900	3.8402	0.2723	0.9873	0.1280
308	3.8774	0.6094	0.9761	0.0615	4.8285	0.1271	0.9822	0.2393
318	3.6245	1.0158	0.9754	0.0378	4.8076	0.0983	0.9455	0.8909
328	3.7202	1.2691	0.9700	0.0305	5.5005	0.0654	0.7636	0.3792

Table 3 lists a comparison of previous maximum adsorption capacities of R6G dye onto different adsorbents, with the highest values obtained using biosorbents in our work.

Table 3: Values of the maximum adsorption capacities Q_m which was reported in the literature for R6G dye using various adsorbents

Adsorbent	Q_m(mg/g)	References
Coffee ground powder	17.3	**7**
Fe_3O_4 nanoparticle composites	9.42	**34**
Activated carbon Particle size (0.5 mm)	11.8	**35**
Activated carbon Particle size (0.71 mm)	6.4	
Activated carbon Particle size (1.0 mm)	4.3	
SD	8.53	**This study**
Phm	5.50	

3.3.2. Freundlich isotherm (FrI) Model:

The **(FrI)** model is used to describe a heterogeneous surface. Figure 14 shows **(FrI)** model of R6G dye onto SD and Phm at various temperatures, and Table 4 shows the values of **(FrI)** constants. It was obvious that the values of R^2 lie between 0.9081- 0.9998 for SD and lie between 0.9481- 0.9884 for Phm, which indicates that the adsorption process was carried out on a heterogeneous surface**.** Furthermore, the values of $(1/n_f)$ are $0 < (1/nf) < 1$, indicating the isotherm is favorable [16].

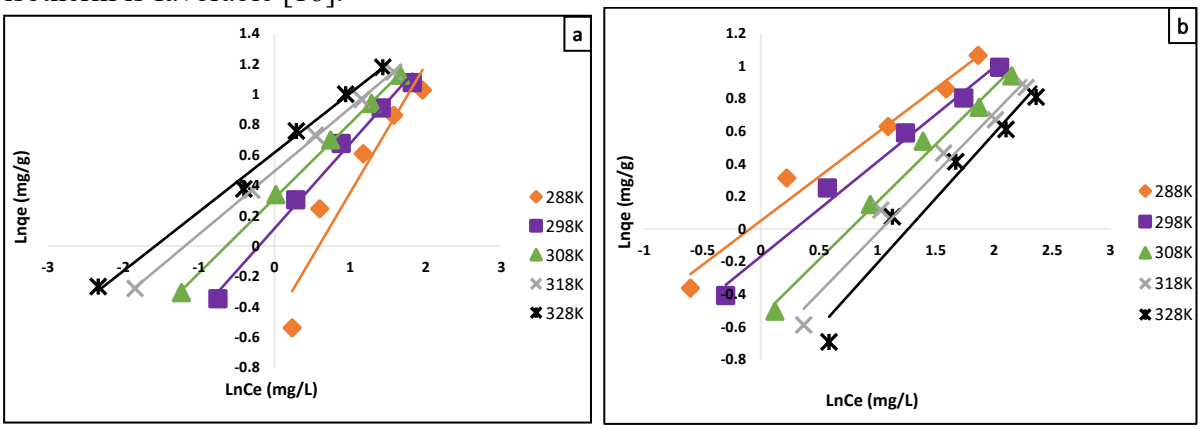

Figure 14. (FrI) model of R6G dye onto (a) SD (b) Phm at various temperatures.

Table 4: (FrI) constants for adsorption of R6G dye onto SD and Phm at various temperatures.

T (K)	SD					Phm				
	$(\frac{1}{n_f})$	n_f	lnK_{Fr}	K_{Fr} $(mg.g^{-1}(mg.L^{-1})^{-1/n})$	R^2	$(\frac{1}{n_f})$	n_f	lnK_{Fr}	K_{Fr} $(mg.g^{-1}(mg.L^{-1})^{-1/n})$	R^2
288	**0.8457**	**1.1824**	**-0.4943**	**0.6099**	**0.9081**	**0.5407**	**1.8495**	**0.0498**	**1.0511**	**0.9756**
298	**0.5596**	**1.7869**	**0.1162**	**1.1232**	**0.9916**	**0.5794**	**1.7259**	**-0.1690**	**0.8448**	**0.9872**
308	**0.4937**	**2.0255**	**0.3151**	**1.3703**	**0.9992**	**0.7057**	**1.4170**	**-0.5406**	**0.5824**	**0.9884**
318	**0.4162**	**2.4026**	**0.4934**	**1.6378**	**0.9998**	**0.7336**	**1.3631**	**-0.7590**	**0.4682**	**0.9741**
328	**0.3904**	**2.5614**	**0.6161**	**1.8516**	**0.9935**	**0.7933**	**1.2606**	**-1.0030**	**0.3668**	**0.9481**

3.4. Adsorption Thermodynamics

Figure 15 presents the Van't Hoff plots for the adsorption of R6G dye onto SD and Phm at various temperatures. The thermodynamic calculations that were estimated for the adsorption

of R6G dye on biosorbents are summarized in Table 5. The negative values of ΔG° at all studied temperatures indicate that the adsorption of R6G dye onto both biosorbents is a spontaneous process. Moreover, the magnitude of ΔG° becomes more negative with increasing temperature, confirming that spontaneity increases with temperature [17]. For SD, both ΔH° and ΔS° were found to be positive. The positive enthalpy change (ΔH° > 0) indicates that the adsorption process is endothermic, while the positive entropy change (ΔS° > 0) suggests an increase in randomness at the solid–solution interface during the adsorption process. In contrast, the negative values of ΔH° and ΔS° obtained for Phm indicate that the adsorption is exothermic and occurs with a decrease in randomness at the solid–liquid interface [36]. Furthermore, the relatively low values of ΔH° for both adsorbents (ΔH° < 40 kJ/mol) suggest that the adsorption of R6G onto SD and Phm is primarily governed by physisorption. The endothermic and exothermic nature of the adsorption of R6G dye onto SD and Phm as adsorbents, as observed from ΔH° values, confirmed the trend which were found in the temperature effect study.

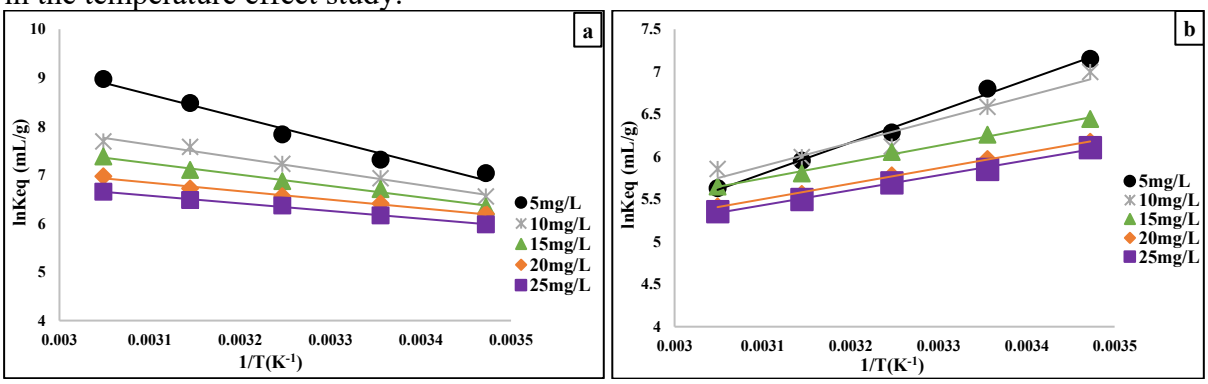

Figure 15: Van't Hoff plots for the adsorption of R6G dye onto (a) SD (b) Phm at various temperatures.

Table 5: Thermodynamic parameters for the adsorption of R6G dye onto SD and Phm at various temperatures.

Adsorbent	C_i (mg/L)	ΔH° (kJ/mol)	ΔS° (kJ/mol.K)	(-) ΔG°(kJ/mol)				
				288K	298K	308K	318K	328K
SD	5	39.433	0.1941	16.843	18.109	20.061	22.407	24.470
	10	23.000	0.1346	15.693	17.175	18.507	20.034	20.968
	15	19.354	0.1201	15.193	16.605	17.584	18.774	20.118
	20	14.568	0.1020	14.835	15.871	16.803	17.759	19.006
	25	13.075	0.0951	14.321	15.269	16.310	17.126	18.148
Phm	5	-30.574	-0.0465	17.120	16.850	16.091	15.737	15.353
	10	-22.820	-0.0217	16.754	16.319	15.666	15.847	15.964
	15	-16.051	-0.0020	15.429	15.500	15.500	15.343	15.401
	20	-15.174	-0.0013	14.788	14.791	14.804	14.705	14.765
	25	-14.649	-0.0002	14.621	14.495	14.575	14.534	14.596

3.5. Kinetics Model

Kinetic studies are critical for adsorption processes, providing vital information on the adsorption rate and controlling the residence time required for process completion. Kinetic experiments were carried out at initial concentrations of R6G dye (5, 10, 15, 20,25 mg. L^{-1}), adsorption time was 5 to 90 min, adsorbent dosage 0.32g/50mL and shaking speed 150 rpm at 298K.

Pseudo 1st model describes the rate of adsorption, which is proportional to the number of unproductive binding sites on adsorbents **[18].** Figure 16 shows the straight line $\ln(q_e - q_t)$

versus (t) for the adsorption of R6G dye onto SD and Phm powder at 298K, and Table 6 shows the pseudo-first model parameters. In this Table, we can observe the values of q_e experimental (q_e exp) are not equal to the values of q_e calculated (q_e cal), the average values of R^2 for SD was (0.9811) and the average values of R^2 for Phm was (0.9828).

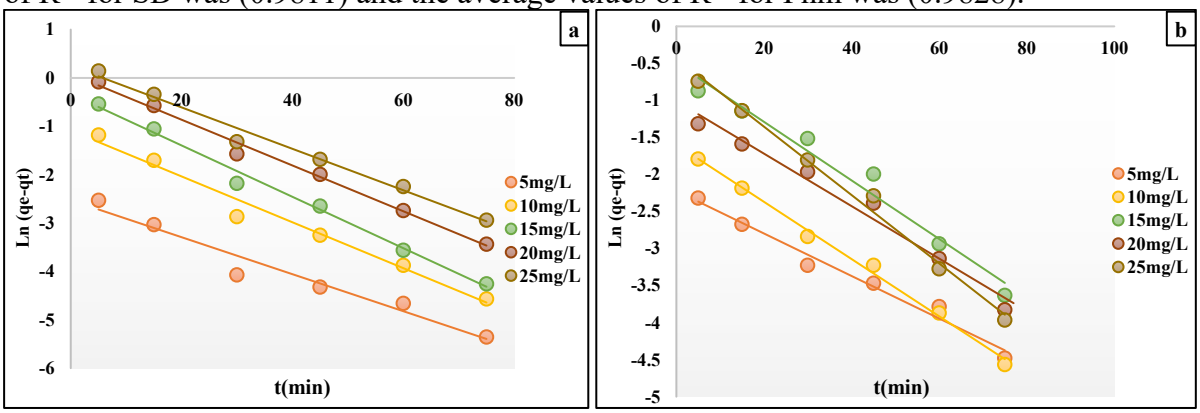

Figure 16: Pseudo 1st model kinetic plots for the adsorption of R6G dye onto (a) SD (b) Phm powder at 298K.

Table 6: Pseudo 1st model rate constants for the adsorption of R6G dye onto SD and Phm at 298K.

C_i (mg/L)	SD				Phm			
	q_e exp (mg/g)	q_e cal (mg/g)	k_1 (min^{-1})	R^2	q_e exp (mg/g)	q_e cal (mg/g)	k_1 (min^{-1})	R^2
5	0.7433	0.0798	0.0382	0.9577	0.6504	0.1083	0.0287	0.9797
10	1.4126	0.3367	0.0474	0.9795	1.2856	0.2026	0.0386	0.9953
15	2.0934	0.7161	0.0531	0.9918	1.9455	0.6080	0.0395	0.9697
20	2.6452	1.0855	0.0473	0.9919	2.4063	0.3643	0.0354	0.9778
25	3.1989	1.2801	0.0428	0.9846	3.0320	0.6501	0.0462	0.9916

Pseudo 2nd model suggested that the rate of the adsorption process is assumed to be linearly correlated with the available vacant sites on the adsorbent's surface**.** Figure 17 shows a linear plot t/q_t against t for the adsorption of R6G dye onto SD and Phm powders at 298K . Table 7 shows the values of the corresponding parameters of pseudo 2nd model and the values of the correlation coefficient. As shown in this Table, the average values of R^2 were (0.9994) for Phm and (0.9997) for SD, the values of q_e experimental (q_e exp) are approximate from the values of q_e calculated (q_e cal). It was noticed from these results that the average values of R^2 for the pseudo 2nd model were higher than the average values of R^2 for pseudo1st model, and the values q_e exp agrees with the values q_e call for pseudo 2nd model. It was observed that the pseudo 1st model did not adequately describe the adsorption process, suggesting that the pseudo 2nd kinetic model is more appropriate for this system. **[37].**

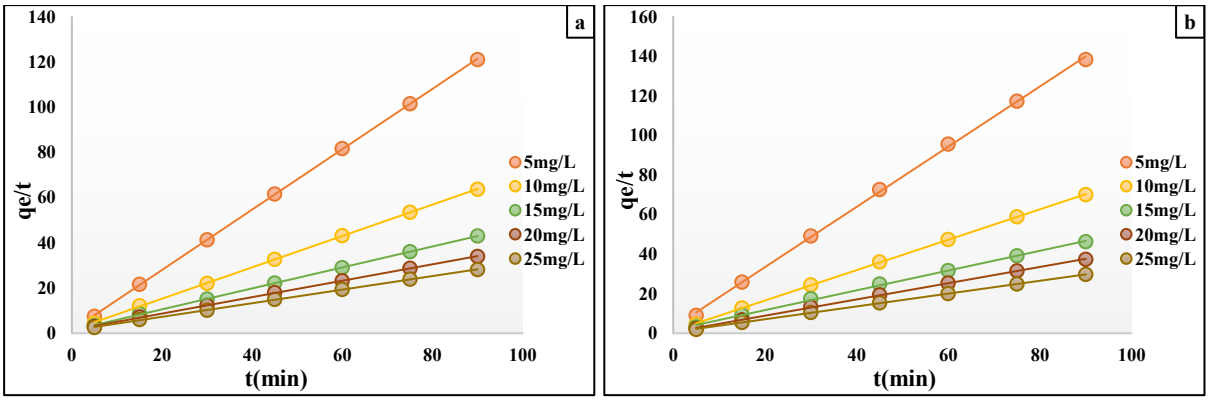

Figure 17: Pseudo 2nd model kinetic plot for the adsorption of R6G dye on (a) SD (b) Phm powder at 298K.

Table 7: Pseudo 2nd model kinetic parameters of the adsorption of R6G dye onto SD and Phm at 298K.

C_i (mg/L)	SD				Phm			
	q_e exp (mg/g)	q_e cal (mg/g)	k_2 (g/mg. min)	R^2	q_e exp (mg/g)	q_e cal (mg/g)	k_2 (g/mg. min)	R^2
5	0.7433	0.7487	1.3717	0.9999	0.6504	0.6563	0.7925	0.9994
10	1.4126	1.4411	0.3417	0.9999	1.2856	1.3003	0.5179	0.9998
15	2.0934	2.1570	0.1655	0.9998	1.9455	1.9980	0.1504	0.9987
20	2.6452	2.7517	0.0919	0.9997	2.4063	2.4324	0.2611	0.9996
25	3.1989	3.3266	0.0714	0.9996	3.0320	3.0826	0.1790	0.9998

Conclusion

The present study highlights that both Phm and SD are promising biosorbents for the removal R6G dye from aqueous solution. AFM measurements revealed that the particle size of SD is smaller than that of Phm, which contributes to the higher removal percentage for SD as an adsorbent, while FT-IR analysis detects the presence of different Functional groups in these samples. The optimum conditions selected are 0.16g as adsorbent weight, 30 min as adsorption period, 10mg/L R6G concentration and pH 7 for both biosorbents. According to Giles Classification, the adsorption of R6G dye onto Phm and SD powder follows the L-Type isotherm and best fits with (FrI) model. Moreover, thermodynamic studies indicate that the adsorption process occurs spontaneously, endothermic in nature occurs with an increase in disorder for SD, while exothermic in nature and occurs with a decrease in disorder for Phm as the adsorbent. Furthermore, the adsorption of R6G dye onto both SD and Phm is a physisorption type. Kinetic results are found to be fitted by the pseudo 2nd model.

References

[1] S. S. Azhar, A. G. Liew, D. Suhardy, K. F. Hafiz, and M. I. Hatim, "Dye removal from aqueous solution by using adsorption on treated sugarcane bagasse," *American Journal of applied sciences*, vol. 2, no. 11, pp. 1499-1503, 2005.

[2] J. Carpenter, S. Sharma, A. K. Sharma, and S. Verma, "Adsorption of dye by using the solid waste from leather industry as an adsorbent," *International Journal of Engineering Science Invention*, vol. 2, no. 1, pp. 1-6, 2013.

[3] R. T. Salim and D. E. AL-Mammar, "Adsorption of Azo Dye onto TiO_2 Nanoparticles Prepared by a Novel Green Method: Isotherm and Thermodynamic Study," *Iraqi Journal of Science*, vol. 64, no. 8, pp. 3779-3792, 2023.

[4] K. Foo and B. H. Hameed, "An overview of dye removal via activated carbon adsorption process," *Desalination and Water Treatment*, vol. 19, no. 1-3, pp. 255-274, 2010.

[5] V. Garg, R. Gupta, A. B. Yadav, and R. Kumar, "Dye removal from aqueous solution by adsorption on treated sawdust," *Bioresource technology*, vol. 89, no. 2, pp. 121-124, 2003.

[6] K. B. Tan, M. Vakili, B. A. Horri, P. E. Poh, A. Z. Abdullah, and B. Salamatinia, "Adsorption of dyes by nanomaterials: recent developments and adsorption mechanisms," *Separation and purification technology*, vol. 150, pp. 229-242, 2015.

[7] K. Shen and M. Gondal, "Removal of hazardous Rhodamine dye from water by adsorption onto exhausted coffee ground," *Journal of Saudi Chemical Society*, vol. 21, pp. S120-S127, 2017.

[8] A. R. Amrin, "Enhensment adsorption capacity of Phragmites australis powder for Congo red and methylene blue dyes removal," *Mesopotamia Environmental Journal*, no. Special Issue C, 2017.

[9] B. T. M. Nguyet, N. H. Nghi, N. A. Tien, D. Q. Khieu, H. D. Duc, and N. Van Hung, "Enhanced Adsorption of Methylene Blue by Chemically Modified Materials Derived from Phragmites australis Stems," *Acta Chimica Slovenica*, vol. 69, no. 4, 2022.

[10] N. S. Sayed, A. S. Ahmed, M. H. Abdallah, and G. A. Gouda, "ZnO@ activated carbon derived from wood sawdust as adsorbent for removal of methyl red and methyl orange from aqueous solutions," *Scientific Reports*, vol. 14, no. 1, p. 5384, 2024.

[11] R. Chikri, N. Elhadiri, M. Benchanaa, and Y. Maguana, "Efficiency of sawdust as low-cost adsorbent for dyes removal," *Journal of Chemistry*, vol. 2020, pp. 1-17, 2020.

[12] G. B. Kankılıç and A. Ü. Metin, "Phragmites australis as a new cellulose source: extraction, characterization and adsorption of methylene blue," *Journal of Molecular Liquids*, vol. 312, p. 113313, 2020.

[13] M. Šćiban, B. Radetić, Ž. Kevrešan, and M. Klašnja, "Adsorption of heavy metals from electroplating wastewater by wood sawdust," *Bioresource technology*, vol. 98, no. 2, pp. 402-409, 2007.

[14] S. P. Hinge, M. S. Orpe, K. V. Sathe, G. D. Tikhe, N. S. Pandey, K. N. Bawankar., M. V. Bagal., A. V. Mohod., & P. R. Gogate., "Combined removal of Rhodamine B and Rhodamine 6G from wastewater using novel treatment approaches based on ultrasonic and ultraviolet irradiations," *Desalination and Water Treatment*, vol. 57, no. 50, pp. 23927-23939, 2016.

[15] A. K. Abaas, D. E. Al-Mammar, and H. A. Abbas, "Equilibrium, Thermodynamic and Kinetic Study of the Adsorption of a New Mono Azo dye onto Natural Iraq Clay," *Journal of Global Pharma Technology*" vol. 10, no. 5, pp. 102-109, 2018. ISSN: 0975 -8542.

[16] N. H. AL-Shammari and D. E. AL-Mammar, "Equilibrium and kinetic modeling studies for the adsorption-desorption of methyl violet 10B onto leather waste," *Eurasian Chemical Communications*, vol. 4, no. 2, pp. 175-189, 2022.

[17] S. S. Mohammed and D. T. Al-Heetimi, "Adsorption of Methyl Violet Dye from Aqueous Solution by Iraqi Bentonite and Surfactant–Modified Iraqi Bentonite," *Ibn AL-Haitham Journal for Pure and Applied Science*, vol. 32, no. 3, pp. 28-42, 2019.

[18] E. Abdul Hussein, S. H. Kareem, and I. H. Ali, "Utilization of Magnetic Mesoporous Silica (Fe_3O_4@$mSiO_2$) in Adsorption, Loading, and Release Kinetics of Diphenhydramine Drug," *Iraqi Journal of Science*, vol. 66, no. 7, pp. 2657–2668, 2025.

[19] B. Nagy, C. Mânzatu, A. Măicăneanu, C. Indolean, L. Silaghi-Dumitrescu, and C. Majdik, "Effect of alkaline and oxidative treatment on sawdust capacity to remove Cd (II) from aqueous solutions: FTIR and AFM study," *Journal of Wood Chemistry and Technology*, vol. 34, no. 4, pp. 301-311, 2014.

[20] D. Nath Barman, M. A. Haque, T. H. Kang, G. H. Kim, T. Y. Kim, M. K. Kim., & H. D. Yun., "Effect of mild alkali pretreatment on structural changes of reed (Phragmites communis Trinius) straw," *Environmental technology*, vol. 35, no. 2, pp. 232-241, 2014.

[21] N. Gao, A. Li, C. Quan, L. Du, and Y. Duan, "TG–FTIR and Py–GC/MS analysis on pyrolysis and combustion of pine sawdust," *Journal of Analytical and Applied Pyrolysis*, vol. 100, pp. 26-32, 2013.

[22] S. Benyoucef, D. Harrache, S. Djaroud, K. Sail, D. Gallart-Mateu, and M. de la Guardia, "Preparation and characterization of novel microstructure cellulosic sawdust material: application as potential adsorbent for wastewater treatment," *Cellulose*, vol. 27, pp. 8169-8180, 2020.

[23] M. A. Moreki, G. G. Matlou, and N. Rapulenyane, "Photo-catalytic degradation of Rhodamine 6G under visible lamp using citrate stabilized ZnO nanoparticles," *Results in Chemistry*, p. 102405, 2025.

[24] P. Senthil Kumar, P. S. A. Fernando, R. T. Ahmed, R. Srinath, M. Priyadharshini, A. Vignesh., & A. Thanjiappan., "Effect of temperature on the adsorption of methylene blue dye onto sulfuric acid–treated orange peel," *Chemical Engineering Communications*, vol. 201, no. 11, pp. 1526-1547, 2014.

[25] M. H. Dehghani, A. Zarei, A. Mesdaghinia, R. Nabizadeh, M. Alimohammadi, and M. Afsharnia, "Response surface modeling, isotherm, thermodynamic and optimization study of arsenic (V) removal from aqueous solutions using modified bentonite-chitosan (MBC)," *Korean Journal of Chemical Engineering*, vol. 34, pp. 757-767, 2017.

[26] H. B. Senturk, D. Ozdes, and C. Duran, "Biosorption of Rhodamine 6G from aqueous solutions onto almond shell (Prunus dulcis) as a low cost biosorbent," *Desalination*, vol. 252, no. 1-3, pp. 81-87, 2010.

[27] S. Ladnorg., N.L. Junior., P. Dall., D.G. Domingos., B.S. Magnus., M. Wichern., T. Gehring., and R.H.R. da Costa., "Alginate-like exopolysaccharide extracted from aerobic granular sludge as biosorbent for methylene blue: Thermodynamic, kinetic and isotherm studies," *Journal of Environmental Chemical Engineering*, vol. 7, no. 3, p. 103081, 2019.

[28] R. A. Mohammed and D. E. Al-Mammar, "Using tobacco leaves as adsorbent for the Orange-G dye removal from its aqueous solutions," *Journal of Global Pharma Technology*, vol. 11, no. 3, pp. 273-280, 2019.

[29] S. Lairini, K. El Mahtal, Y. Miyah, K. Tanji, S. Guissi, S. Boumchita., & F. Zerrouq., "The adsorption of Crystal violet from aqueous solution by using potato peels (Solanum tuberosum): equilibrium and kinetic studies," *Journal of Materials and Environmental Science*, vol. 8, no. 9, pp. 3252-3261, 2017.

[30] S. Laghrib, C. E. Gherdaoui, O. Belgherbi, N. Benaskeur, M. Boudissa, A. Kanagaraj, & N. Aouffa., "Photocatalytic degradation of methylene blue using TiO2 nanoparticles synthesized via the sol–gel method in acidic and neutral media," *Reaction Kinetics, Mechanisms and Catalysis*, pp. 1-21, 2025.

[31] Q. Hu and Z. Zhang, "Application of Dubinin–Radushkevich isotherm model at the solid/solution interface: A theoretical analysis," *Journal of Molecular Liquids*, vol. 277, pp. 646-648, 2019.

[32] J. S. Piccin, T. R. S. A. Cadaval, L. A. A. De Pinto, and G. L. Dotto, "Adsorption isotherms in liquid phase: experimental, modeling, and interpretations," *Adsorption processes for water treatment and purification*, pp. 19-51, 2017.

[33] B. Hameed, I. Tan, and A. Ahmad, "Adsorption isotherm, kinetic modeling and mechanism of 2, 4, 6-trichlorophenol on coconut husk-based activated carbon," *Chemical engineering journal*, vol. 144, no. 2, pp. 235-244, 2008.

[34] T. Suwunwong, P. Patho, P. Choto, and K. Phoungthong, "Enhancement the rhodamine 6G adsorption property on Fe3O4-composited biochar derived from rice husk," *Materials Research Express*, vol. 7, no. 2, p. 025511, 2020.

[35] G. Annadurai, R.-S. Juang, and D.-J. Lee, "Adsorption of rhodamine 6G from aqueous solutions on activated carbon," *Journal of Environmental Science and Health*, Part A, vol. 36, no. 5, pp. 715-725, 2001.

[36] M. H. Dehghani, A. Zarei, A. Mesdaghinia, R. Nabizadeh, M. Alimohammadi, and M. Afsharnia, "Response surface modeling, isotherm, thermodynamic and optimization study of arsenic (V) removal from aqueous solutions using modified bentonite-chitosan (MBC)," *Korean Journal of Chemical Engineering*, vol. 34, pp. 757-767, 2017.

[37] V. D. Pakhale and P. R. Gogate, "Removal of rhodamine 6g from industrial wastewater using combination approach of adsorption followed by sonication," *Arabian Journal for Science and Engineering*, vol. 46, pp. 6473-6484, 2021.